Physics of the Solid State, Vol. 44, No. 1, 2002, pp. 164–170. Translated from Fizika Tverdogo Tela, Vol. 44, No. 1, 2002, pp. 157–164.
Original Russian Text Copyright © 2002 by Vyalykh, Shikin, Prudnikova, Grigor'ev, Starodubov, Adamchuk.

LOW-DIMENSIONAL SYSTEMS AND SURFACE PHYSICS

Quantum-Well States and Resonances in Thin Single-Crystal Layers of Noble Metals on W(110) Substrates

D. V. Vyalykh[1, 2], A. M. Shikin[1], G. V. Prudnikova[1], A. Yu. Grigor'ev[1, 2],
A. G. Starodubov[1], and V. K. Adamchuk[1]

[1] *Institute of Physics (Petrodvorets Branch), St. Petersburg State University,*
ul. Pervogo maya 100, Petrodvorets, 198904 Russia
e-mail: vyalikh@paloma.spbu.ru
e-mail: prudnikg@paloma.spbu.ru
[2] *Free University of Berlin, Arnimalle 14, 14195 Berlin-Dahlem, Federal Republic of Germany*

Received March 15, 2001; in final form, May 7, 2001

Abstract—This paper reports on the first experimental observation of quantum-well states and *sp*-type resonances in thin single-crystal gold, silver, and copper layers formed on single-crystal W(110) surfaces, which result from spatial localization of Bloch-type electronic wave functions in a quantum well with potential barriers at the vacuum/metal and metal/W(110) interfaces. The quantization of the valence-band electronic structure in Au/W(110), Ag/W(110), and Cu/W(110) systems was studied experimentally using angle-resolved photoelectron spectroscopy. *© 2002 MAIK "Nauka/Interperiodica".*

1. INTRODUCTION

Research in modern solid-state physics focuses considerable attention on the experimental study and theoretical analysis of the electronic structure in low-dimensional systems. This interest is accounted for, on the one hand, by the lack of information on such structures compared, e.g., to bulk crystals and, on the other, by the broad application potential of low-dimensional systems in micro- and nanoelectronics. In thin layers, the motion of electrons perpendicular to the surface of a solid is substantially constrained, with the scale of this limitation being comparable to the coherence length of the electron wave function. As a result of the electron motion being constrained in this direction, the energy spectrum becomes modified and the continuum typical of a bulk crystal is replaced by a set of quantum-well states (QWSs). A QWS standing wave is produced through the interference of Bloch electronic waves, which are multiply reflected from the walls of the potential well formed by the vacuum/metal and metal/substrate interfaces. Note that the actual energy position of the QWS depends on the potential well width, i.e., on the thickness of the quasi-two-dimensional structure [1]. Therefore, dispersion in the spectral features of the thin-film system under study with variation of its thickness serves as evidence of the existence of the QWS. The quantization of the electronic energy bands of a bulk single crystal occurring as one crosses over to thin single-crystal films offers a unique possibility of using angle-resolved photoelectron spectroscopy (ARPES) to experimentally study the quantum electronic states created in thin metal layers [1, 2]. The most essential goal of these experimental studies was to obtain thin single-crystal films of noble metals with a perfect crystal structure, because any defects at the vacuum/metal and metal/W(110) interfaces, as well as film inhomogeneities, produce electron scattering and, as a consequence, weaken the effect to be observed. In our experiments, thin single-crystal films were prepared through thermal deposition of noble metals on an atomically clean W(110) surface. The crystal structure of the layers thus produced was analyzed using low-energy electron diffraction (LEED).

Earlier experiments showed [3–7] that the surface of the closely packed (111) face of a thin fcc metal layer formed on the (110) surface of a bcc metal can have two

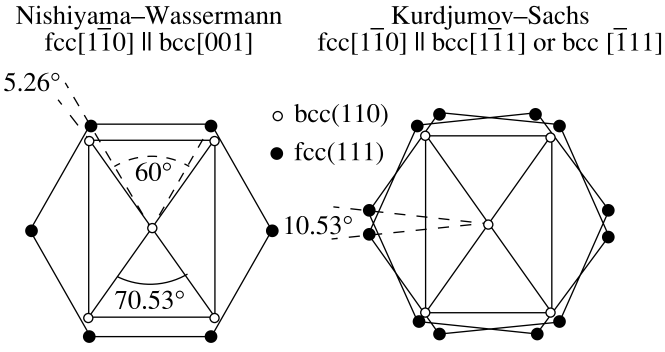

Fig. 1. Two possible (Nishiyama–Wassermann and Kurdjumov–Sachs [7]) orientations of the (111) surface of an fcc metal on the (110) surface of a bcc metal.

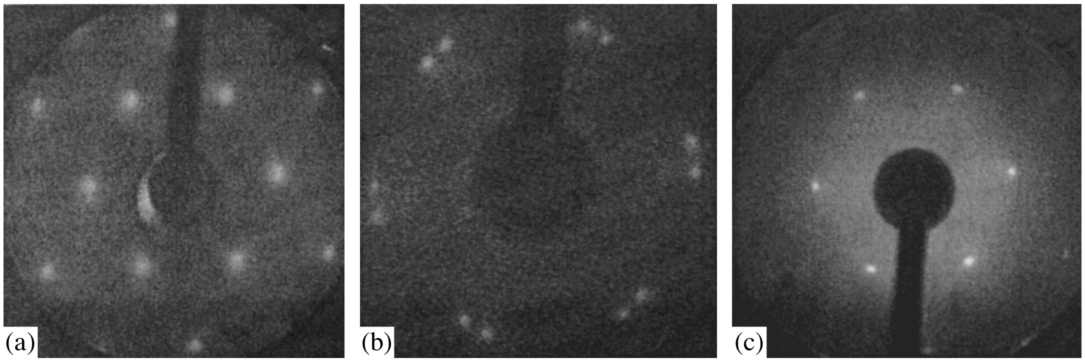

Fig. 2. LEEDS patterns obtained for (a) Au/W(110), E_p = 141 eV; (b) Ag/W(110), E_p = 121 eV; and (c) Cu/W(110), E_p = 173 eV.

types of orientation, Nishiyama–Wassermann (NW) or Kurdjumov–Sachs (KS) [5–7] (Fig. 1), depending on certain conditions (the relative magnitudes of the substrate and adsorbate interatomic distances, film thickness, temperature, etc. [3, 4]). The LEED patterns obtained for the Au/W(110), Ag/W(110), and Cu/W(110) systems (Fig. 2) confirm the formation of thin single-crystal films of Au, Ag, and Cu on the single-crystal W(110) surface. The LEED patterns permit one to conclude that thin Au and Cu layers form through the NW mechanism and Ag layers form through the KS mechanism, which is in agreement with [8].

Our photoemission studies showed that quantum states and resonances of the *sp* type indeed form in Au/W(110), Ag/W(110), and Cu/W(110) structures. It was demonstrated that the photoelectron (PE) spectra observed in the Ag/W(110) system can be employed to monitor the thickness of the deposited layers. The dispersion relation $E(\mathbf{k}_\perp)$ was obtained experimentally for the Cu/W(110) system in the [111] direction.

2. EXPERIMENTAL TECHNIQUE

The studies were carried out at the BESSY-I and BESSY-II synchrotron centers (Berlin, Germany), with output channels TGM3 and U125, respectively, using a WSW ARIES-type angle-resolved electron spectrometer equipped with a diffractometer to measure LEED patterns. Laboratory studies were performed on an SES 200 SCIENTA electron spectrometer with a gas-discharge helium lamp providing $h\nu$ = 21.2 and 40.8 eV photons for ARPES experiments. The total energy resolution reached in the ARPES experiments was ≈150 and ≈50 meV for the ARIES and SCIENTA electron spectrometers, respectively.

The atomically clean W(110) single-crystal surface was obtained through a series of short heatings of the crystal to 2300°C, with subsequent annealing at 1300°C in an oxygen environment in a vacuum of no worse than 5×10^{-8} Torr. The heating in oxygen resulted in a chemical reaction of the oxygen with the carbon evolved onto the W(110) surface from the bulk of the crystal, and the CO_2 thus formed escaped from the surface and was pumped out. This procedure produced an atomically clean W(110) surface, whose quality was monitored using ARPES and LEED. Figure 3 presents a PE spectrum and a LEED pattern characteristic of a perfectly clean W(110) single-crystal surface, which demonstrate the absence of any foreign inclusions on the surface.

Thin single-crystal layers of Au, Ag, and Cu on W(110) substrates were prepared through thermal evaporation of a small piece of the corresponding metal (a sphere ~2–3 mm in diameter, metal purity 99.999%) spot welded to a 0.25-mm diameter wire of W75-Re25 alloy. The wire with the metal was heated to the metal evaporation temperature by passing a dc current through it (~2.7 A for Ag, and ~3.8 A for Au and Cu). The Au, Ag, and Cu single-crystal layers were found to have the best quality when the deposition on a W(110) substrate was made at room temperature at a rate of no more than 2 Å per minute. The thickness of the deposited Au, Ag, and Cu layers was determined from the change in the frequency of a quartz resonator maintained inside the vacuum chamber under the same conditions as the sample. On reaching the base vacuum in the chamber, each source was outgassed to achieve cleanness of the source components, for which the pressure during the evaporator operation increased only to 2×10^{-10} Torr. The base pressure in the chamber in each experiment was kept below 1×10^{-10} Torr.

3. EXPERIMENTAL RESULTS AND DISCUSSION

3.1. Quantum Resonance States in the Au(111)/W(110) System

Figure 4 presents the photoemission spectrum obtained at a photon energy $h\nu$ = 50 eV under normal electron emission from the Au/W(110) system with a gold layer 22 Å thick. This spectrum exhibits several features (denoted by the symbols *2–6*, D_1–D_3, and *S*) that were observed earlier [9, 10]. The feature at 0.4 eV below the Fermi level, which is denoted by S_1, is a Shockley-type surface state located in the relative

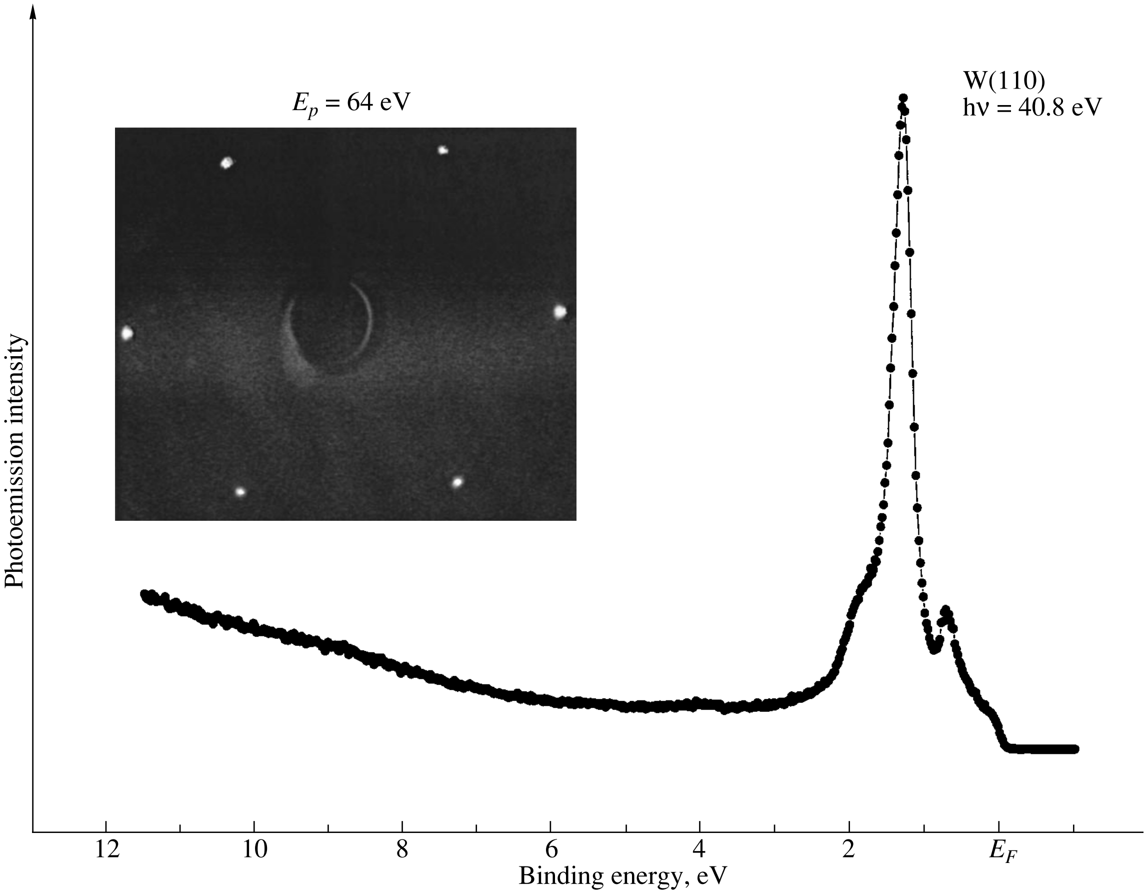

Fig. 3. Photoelectron valence-band spectrum of W(110) measured under normal photoelectron emission and incident photon energy *h*ν = 40.8 eV. Inset: LEED pattern for the W(110) single-crystal surface.

energy gap at the *L* point [10, 11]: $E_F < E_{SS} < 1.1$ eV. The S_2 feature is also assigned to a Shockley-type surface state. This feature was observed earlier in [11] and is in agreement with the surface-state calculations performed for Au(111) in [12]. The symmetric shape of the surface-state peaks and their high intensity argues for the high quality of the Au film. The *2–6* features result from direct transitions between the volume electronic states along the Γ*L* direction. The D_1–D_3 features were shown [9] to be surface resonances, because their energy does not change with varying the photon energy and they exhibit resonance properties at photon energies from 18.6 to 26.5 eV [9]. The *S* feature in the PE spectrum is accounted for by the variation in the potential at the surface [9]. In addition, the PE spectrum also has two new features lying at ≈1.3 and ≈2.0 eV below the Fermi level (denoted by QWR_1 and QWR_2, respectively) that were not observed earlier in the PE spectra obtained when studying bulk single-crystal Au(111) [10]. To establish the nature of these electronic states, we measured PE spectra for different gold layer thicknesses and photon energies. Figure 5 presents PE spectra for the Au/W(110) system obtained at a photon energy *h*ν = 60 eV. The gold layer thickness was varied from 8 to 30 Å. Note that at gold layer thicknesses in excess of 8 Å, a QWR_1 feature appears in the spectrum that shifts toward lower binding energies (toward the Fermi level) with increasing layer thickness. At a gold layer thickness of 18 Å, a QWR_2 feature is seen to appear in the PE spectrum that also changes its energy with increasing film thickness. Note that the QWR_1 and QWR_2 features for the gold layer thickness of 22 Å lie at binding energies of ~1.3 and ~2.0 eV, respectively, which coincide with the positions of similar features in the PE spectrum for the same system measured at a photon energy *h*ν = 50 eV. It should be pointed out that, as the gold layer thickness increases, the QWR_1 and QWR_2 features are observed in the PE spectra at energies down to an energy of ~1.1 eV below the Fermi level (the Au valence-band top in the [111] direction), but their intensities decrease noticeably as one approaches this energy. At binding energies of less than ~1.1 eV, these features are not seen.

The QWR_1 and QWR_2 features observed in the PE spectra cannot be due to surface resonance states, because although their positions are seen to be independent of the photon energy, they change with varying

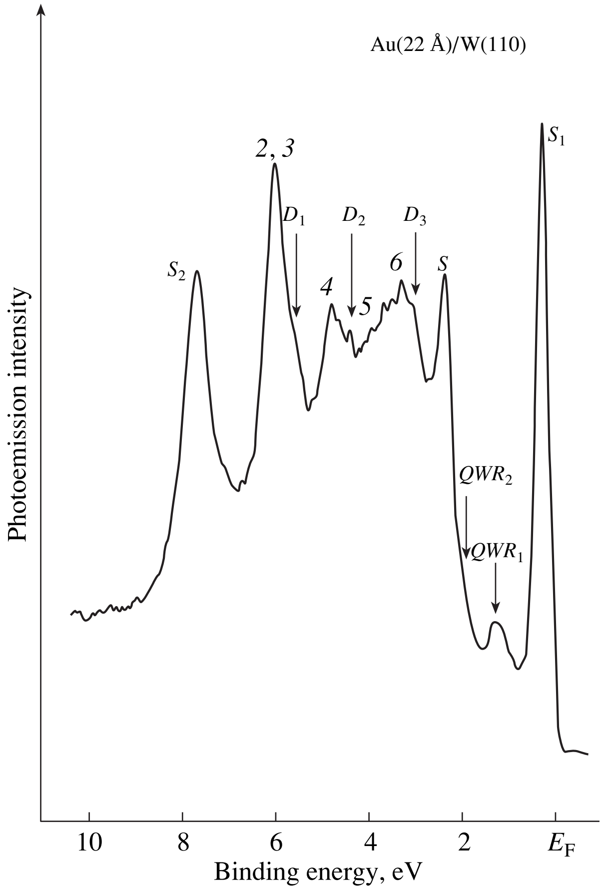

Fig. 4. Photoelectron valence-band spectrum of the Au/W(110) system measured under normal photoelectron emission and incident photon energy $h\nu = 50$ eV. Gold layer thickness 22 Å.

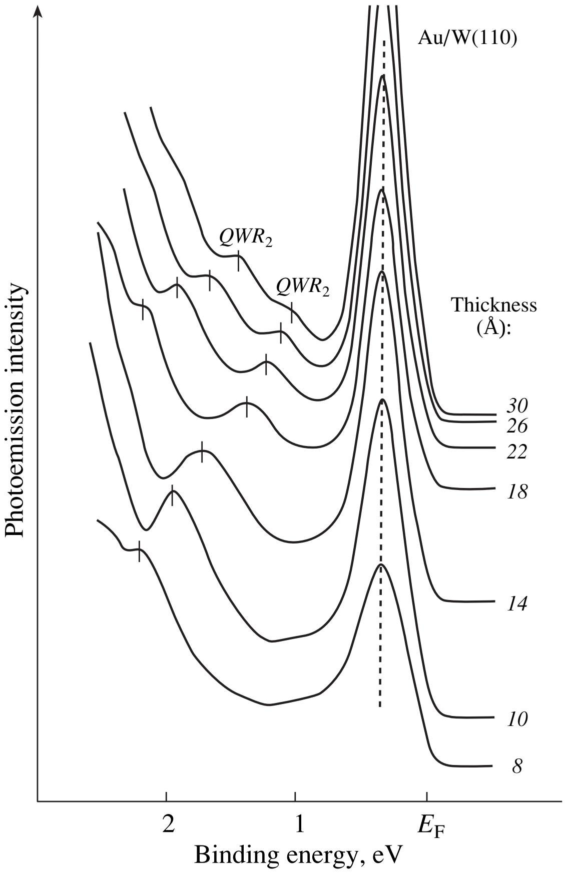

Fig. 5. Photoelectron valence-band spectra of the Au/W(110) system measured for different gold layer thicknesses. The spectra were obtained under normal photoelectron emission and incident photon energy $h\nu = 60$ eV. Dashed line specifies the position of the surface state.

gold layer thickness. For the same reason, QWR_1 and QWR_2 cannot result from hybridization of the Au and W electronic states. We believe that these specific features in the PE spectrum [compared to the PE spectrum of a bulk Au(111) single crystal] can be only a signature of *sp*-type quantum electronic states due to *sp* electrons being spatially confined to a thin single-crystal layer of gold by potential barriers at the Au/vacuum and Au/W interfaces. Tungsten has a relative gap extending from 3.5 to 6.2 eV below the Fermi level in the Γ*N* direction perpendicular to the surface [13, 14]. Because the energy bands Λ_6^1 and Σ_5^2 of gold and tungsten, respectively, have different crystal symmetries [15], the wave functions of the electronic *sp* states in gold will experience practically total reflection from the Au/W interface at energies from 2.0 to 6.2 eV. However, the wave functions of the Au *sp* electrons at binding energies of less than 2.0 eV can penetrate through the effective Au/W potential barrier to interact with the Σ_5^1 electronic states of tungsten [16, 17]. This means that the Au *sp* electron wave functions in this energy region are not totally localized in a thin single-crystal Au layer. Thus, the semiconfined electronic states observed in the PE spectra are *sp*-type quantum resonance states of Au. In the description of quantum resonance states [1], one observes a certain analogy to surface resonance states [9, 18].

Thus, the above analysis gives one grounds to conclude that thin epitaxial Au layers produced on single-crystal W(110) exhibit, in addition to known features, *sp*-type quantum resonance states. Note that the electronic structures of ultrathin gold layers on W(110) substrates were already studied in [17] and *d*-type quantum states were observed at energies from 2 to 4 eV, i.e., in the region of the W energy gap for electronic states in the Γ*N* direction of the Brillouin zone that exhibit Σ_5^1 crystal symmetry.

Note that when the Au/W(110) system is excited by photons of energy $h\nu = 21.2$ eV, the QWR_1 and QWR_2 quantum resonance states are not observed in the PE spectrum, because the electron photoionization cross section is considerably smaller in this case than that for *h*ν = 60 eV. For this reason, quantum resonance states of the *sp* type were not observed in the studies in [17].

3.2. Quantum-Well States and Resonances in the Ag/W(110) System

Figure 6 displays a series of PE spectra measured at a photon energy *h*ν = 50 eV in a system prepared by depositing thin silver layers of various thicknesses onto a W(110) single crystal. For a layer thickness of 2 Å, the PE spectrum exhibits a feature in the region of the *sp* electron binding energy of ≈3.2 eV that can be associated with electron emission from a quantum state characteristic of a monolayer Ag film. As the silver thickness is increased gradually, a new feature appears in the PE spectrum at a binding energy of ≈2.4 eV, which signals the formation of a second monolayer. After the silver coating thickness reaches 7 Å, a feature with a binding energy of ≈2.0 eV is seen to appear in the spectrum, thus indicating the formation of the third monolayer.

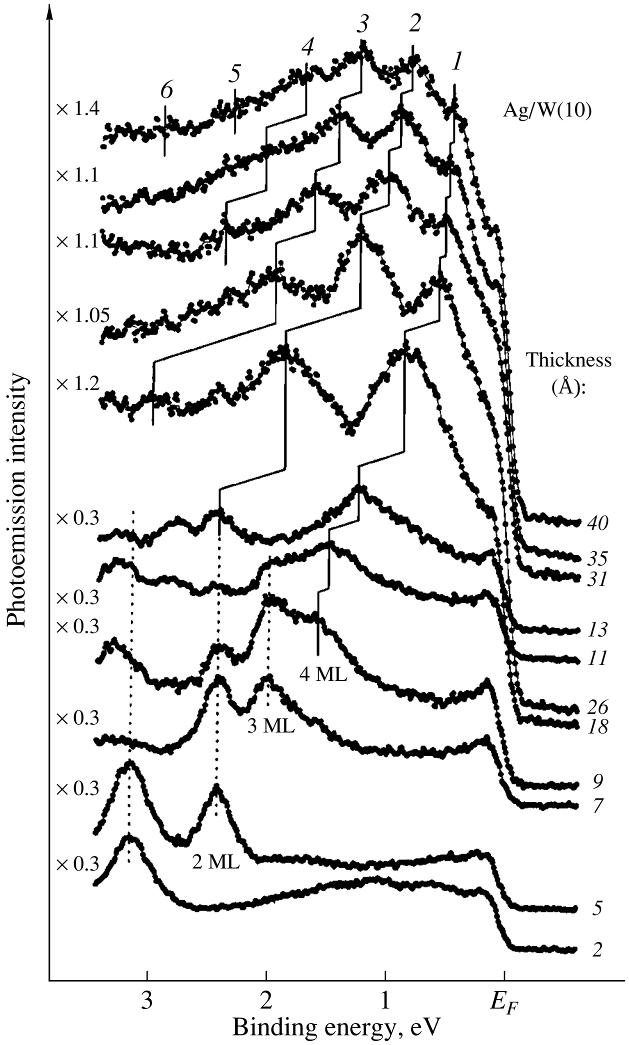

Fig. 6. Photoelectron valence-band spectra of the Ag/W(110) system measured for different silver layer thicknesses. The spectra were obtained under normal photoelectron emission and incident photon energy, *h*ν = 50 eV.

Note that at silver film thicknesses above three monolayers, the film growth was shown to be accompanied by island formation on the surface [8]. This observation is supported by the considerable decrease in intensity of the spectral features originating from quantum states in thicker Ag layers. As a result of the presence of Ag surface imperfections in such films, electrons scatter from surface defects in reflection from the Ag/vacuum interface, thus giving rise to a blurred structure of the PE spectra associated with size quantization.

As in the Au/W(110) system, at binding energies of less than 2 eV, electron wave functions of silver can penetrate through the effective barrier into the substrate. Therefore, the quantum states of silver in this energy region should be considered to be *sp*-type resonance quantum states. Figure 7 plots the typical dependence of the energy positions of the quantum states and resonances on the silver layer thickness.

As seen from Fig. 6, the thickness of a silver layer can be derived from the position of the quantum electronic states in the PE spectra. This experimental observation offers the possibility of using QWSs to determine

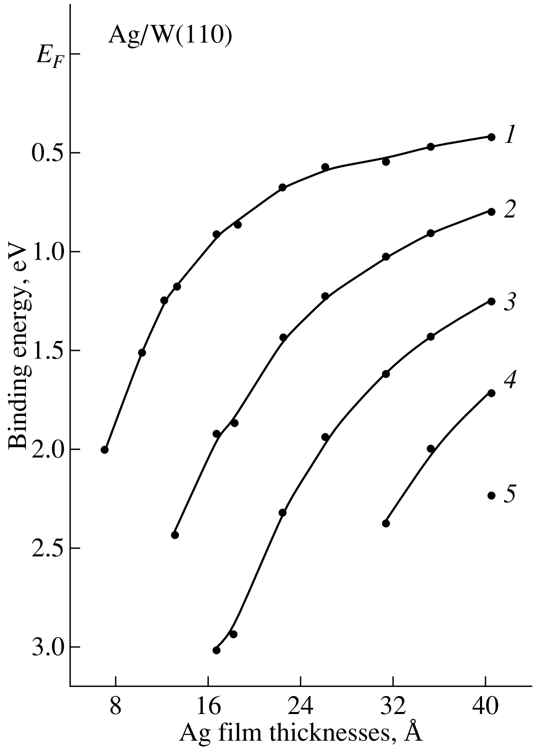

Fig. 7. Energy position of the peaks of quantum states vs. silver film thickness for the Ag/W(110) system derived from the photoelectron spectra in Fig. 6.

the thickness of very thin metal layers in addition to evaporator calibration.

3.3. Quantum Resonance States in the Cu/W(110) System

Interest in this system has been stimulated, on the one hand, by studies of the quantum effects in such systems as, for instance, Cu/Ni(100) [19] and Cu/Co(100) [20], and, on the other, by observations arguing for the existence of *sp*-type quantum resonance states in thin copper layers on W(110), namely, by the possibility of growing thin epitaxial single-crystal copper layers on W(110) substrates [21], by the similarity of the electronic band structures in Au, Ag, and Cu in the [111] direction [15], and by the existence of an effective potential barrier at the Cu/W interface.

Figure 8a displays a series of PE spectra of epitaxial copper films of various thicknesses on W(110) substrates measured at a photon energy $h\nu = 21.2$ eV. At this photon energy, one observes the maximum intensity of the Shockley-type surface state on Cu(110), which provides a possibility of monitoring the surface quality of thin single-crystal copper layers. The feature corresponding to a surface state in the PE spectra shown is observed at a binding energy of ≈0.3 eV below the Fermi level and lies in the energy gap ($E_F < E_{SS} <$ 0.75 eV) at the *L* point. In addition to the surface state, the PE spectrum exhibits a number of features (denoted by *1*–*4*) not seen in the PE spectra of bulk Cu(110) sin-

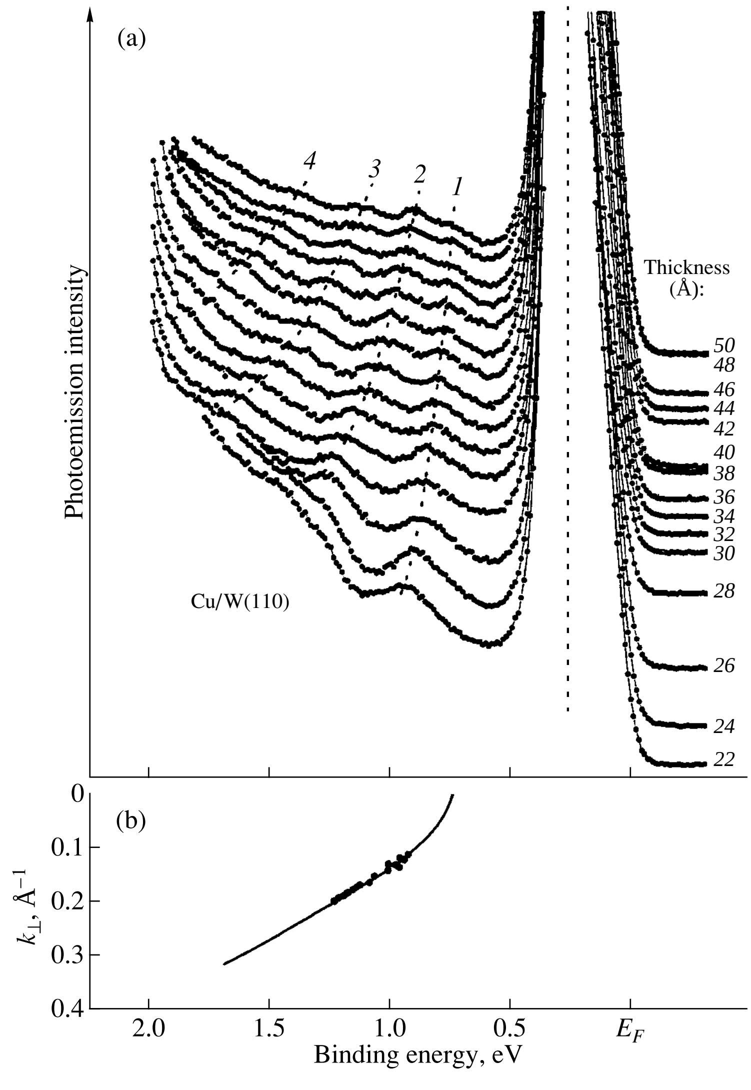

Fig. 8. (a) Valence-band photoelectron spectra of the Cu/W(110) system measured for various copper layer thicknesses; the spectra were obtained under normal photoelectron emission and incident photon energy, $h\nu = 21.2$ eV; the Cu layer thickness is varied from 22 to 50 Å; the dashed line identifies the position of the surface state. (b) Dispersion relation $E(\mathbf{k}_\perp)$ along the [111] direction perpendicular to the Cu(111) surface; points are experimental data extracted from the PE spectra; the solid curve represents a fitting function calculated from the two-band model [25].

gle crystals [22]. Increasing the copper thickness shifts these features toward the Fermi level. These features can be accounted for in terms of the quantization of the Cu *sp* band in the ΓL direction through the formation of quantum electronic states. In the Cu/W(110) system, the wave functions of copper electrons with energies in the range $0.75 < E < 2$ eV are capable of penetrating through the effective Cu/W barrier into the substrate to form semiconfined resonance quantum states.

The quasi-wave vector $\mathbf{k}_\perp$ in the direction perpendicular to the surface for a quantum state with a given energy can be calculated from the condition of quantization of $\mathbf{k}_\perp$, which is based on the finite thickness of a thin layer [1, 23, 24]. Thus, experimental PE spectra can be used to calculate the dispersion relation $E(\mathbf{k}_\perp)$ along the [111] direction. The $E(\mathbf{k}_\perp)$ dispersion for the Cu(111)/W(110) system is presented in Fig. 8b as a set of experimental dots and a curve representing the fitting function $E(\mathbf{k}_\perp)$ calculated in [23] in terms of the two-band model [1, 25]. The best fit to the experimental data was obtained with the following parameters: a copper valence-band top in the given direction of 0.75 eV and an effective mass $m^* = 0.66m_e$, where m_e is the free-electron mass.

4. CONCLUSIONS

Thus, the results of our study of thin single-crystal Au, Ag, and Cu layers formed at room temperature on atomically clean W(110) single-crystal surfaces permit one to conclude that localization of the *sp* electron wave functions gives rise to the formation of quantum-well states and resonances, which reveal characteristic variations of the energy position with metal layer thickness. The quantum states observed in the PE spectra of thin uniform Ag layers on W(110) are a signature of the layer-by-layer film growth, which can be used to measure the thickness of a deposited coating. It should be pointed out that quantum-well states and resonances were observed in the Au/W(110), Ag/W(110), and Cu/W(110) systems for the first time.

ACKNOWLEDGMENTS

The authors express their gratitude to the administration and personnel of the BESSY-I and BESSY-II Synchrotron Radiation Centers for the opportunity to carry out photoemission studies with the use of synchrotron radiation. The authors warmly thank Prof. G. Kaindl and E. Weschke of the *Free* University of Berlin, as well as O. Rader of BESSY-II, for the possibility of using their equipment in the photoemission experiments and for useful discussions.

This study was supported by the State Program "Topical Problems in Condensed-Matter Physics" (Subprogram "Surface Atomic Structures," project no. 2.1-99), the Russian Foundation for Basic Research (project no. 01-02-17287), and also by the DFG (grant Sfb-290/TPA06) and BMBF (grant 05 SF8 KEC8) (Germany).

REFERENCES

1. T. C. Chiang, Surf. Sci. Rep. **39**, 181 (2000).
2. F. J. Himpsel, J. E. Ortega, G. J. Mankey, and R. F. Willis, Adv. Phys. **47** (4), 511 (1998).
3. Y. Goth, M. Uwaha, and I. Arai, Appl. Surf. Sci. **33/34**, 443 (1988).
4. E. Bauer and J. van der Werwe, Phys. Rev. B **33**, 3657 (1986).
5. Z. Nishiyma, Sci. Rep. Tohoku Univ. **23**, 658 (1934).
6. G. Kurdjumov and G. Shachs, Z. Phys. **64**, 325 (1930).
7. O. Hellwig, K. Theis-Brohl, G. Wihelmi, and H. Zabel, Surf. Sci. **410**, 362 (1998).
8. E. Bauer, H. Poppa, G. Todd, and P. R. Davis, J. Appl. Phys. **48**, 3773 (1977).
9. H. G. Zimmer and A. Goldmann, Surf. Sci. **176**, 115 (1986).
10. S. D. Kevan and R. Gaylord, Phys. Rev. B **36**, 5809 (1987).
11. R. Courths, H. Wern, U. Hau, *et al.*, J. Phys. F **14**, 1559 (1984).
12. S. H. Liu, C. Hinnen, C. C. Nguyen van Huong, *et al.*, J. Electronanal. Chem. **176**, 325 (1984).
13. D. Li, P. A. Dowben, J. E. Ortega, and F. J. Himpsel, Phys. Rev. B **47**, 12895 (1993).
14. J. Feydt, A. Elbe, H. Engelhard, *et al.*, Phys. Rev. B **58**, 14007 (1998).
15. H. Eckardt, L. Fritsche, and J. Noffke, J. Phys. F **14**, 97 (1984).
16. R. H. Gaylord and S. D. Kevan, Phys. Rev. B **36**, 9337 (1987).
17. H. Knoppe and E. Bauer, Phys. Rev. B **48**, 5621 (1993).
18. R. Courths, H.-G. Zimmer, A. Goldmann, and H. Saalfeld, Phys. Rev. B **34**, 33585 (1986).
19. H. Iwasaki, B. T. Jonker, and R. L. Park, Phys. Rev. B **32**, 643 (1985).
20. J. E. Ortega, F. J. Himpsel, G. J. Mankey, and R. F. Willis, Phys. Rev. B **47**, 1540 (1993).
21. K. Reshoft, C. Jensen, and U. Kohler, Surf. Sci. **421**, 320 (1999).
22. S. D. Kevan and R. G. Gaylord, Phys. Rev. Lett. **57**, 2975 (1986).
23. M. A. Mueller, T. Miller, and T.-G. Chiang, Phys. Rev. B **41**, 5214 (1990).
24. A. M. Shikin, D. V. Vyalikh, Yu. S. Dedkov, *et al.*, Phys. Rev. B **62**, R2303 (2000).
25. N. V. Smith, Phys. Rev. B **32**, 3549 (1985).

Translated by G. Skrebtsov